Available online at www.sciencedirect.com
ScienceDirect
Journal of Solid State Chemistry 179 (2006) 3704–3708
JOURNAL OF SOLID STATE CHEMISTRY
www.elsevier.com/locate/jssc

# Electronic structure and visible light photocatalysis water splitting property of chromium-doped $SrTiO_3$

J.W. Liu[a,b], G. Chen[a,*], Z.H. Li[a,c], Z.G. Zhang[b]

[a]*Department of Applied Chemistry, Harbin Institute of Technology, 92 West Dazhi Street, Harbin 150001, PR China*
[b]*Department of Physics, Harbin Institute of Technology, Harbin 150001, PR China*
[c]*State Key Laboratory of Inorganic Synthesis and Preparative Chemistry, Jilin University, Changchun 130023, PR China*

Received 10 April 2006; received in revised form 19 July 2006; accepted 7 August 2006
Available online 30 August 2006

**Abstract**

Cr-doped $SrTi_{1-x}Cr_xO_3$ ($x = 0.00$, 0.02, 0.05, 0.10) powders, prepared by solvothermal method, were further characterized by ultraviolet–visible (UV–vis) absorption spectroscopy. The UV–vis spectra indicate that the $SrTi_{1-x}Cr_xO_3$ powders can absorb not only UV light like pure $SrTiO_3$ powder but also the visible-light spectrum ($\lambda > 420$ nm). The results of density functional theory (DFT) calculation illuminate that the visible-light absorption bands in the $SrTi_{1-x}Cr_xO_3$ catalyst are attributed to the band transition from the Cr 3*d* to the Cr 3*d* + Ti 3*d* hybrid orbital. The photocatalytic activities of chromium-doped $SrTiO_3$ both under UV and visible light are increased with the increase in the amounts of chromium.


*Keywords:* Water splitting; Solvothermal; Photocatalysis

## 1. Introduction

Much attention has been paid to photocatalytic water splitting because of its potential to obtain directly clean and high-energy containing $H_2$ from abundant $H_2O$ [1–5]. Although there has been remarkable progress in recent decades for photocatalysts working under ultraviolet (UV) light, this progress has rarely extended to the visible light region [6]. Doping with transition metal ions, such as chromium and iron, has been demonstrated to be an efficient way to develop new visible-light-driven photocatalysts [7–11].

$SrTiO_3$, as one of the most promising photocatalysts, is now used in various practical applications [12–16]. However, the majority of syntheses of the photocatalysts to date has been carried out using the conventional solid-state reaction (SSR) route at high temperatures (typically 1000–1200 °C) [17–20]. Common problems in the SSR route include the uncontrollably large grain growth, localized segregation of one or more components, and possible loss of stoichiometry due to volatilization of the constituent components at high temperatures, all of which result in a decrease in the photocatalytic activity of a given catalyst to a great extent. The solvothermal method seems to be promising due to the ability to control chemical homogeneity, purity, morphology, shape and phase composition of the powders under moderate conditions.

The principal aim of this paper is to demonstrate the feasibility of the solvothermal method for the low-temperature (100 °C) synthesis of $SrTiO_3$ and chromium-doped $SrTiO_3$ materials with visible light response photocatalytic activities. The band structures of $SrTiO_3$ and chromium-doped $SrTiO_3$ were also discussed on the basis of density functional theory (DFT) calculations.

## 2. Experimental section

Tetrabutyl titanate ($C_{16}H_{36}O_4Ti$), $Sr(NO_3)_2$, ethanol (analytical reagents grade, AR) were used as the starting materials. In a typical process, tetrabutyl titanate was solved in 5 mL ethanol with stirring. After 10 min, a solution of $Sr(NO_3)_2$ in 5 mL deionized water was added and the mixture was stirred for 2 h, which caused the

*Corresponding author. Fax: +86 451 86413753.
*E-mail address:* gchen@hit.edu.cn (G. Chen).

0022-4596/$ - see front matter © 2006 Elsevier Inc. All rights reserved.
doi:10.1016/j.jssc.2006.08.014

immediate precipitation of a white solid. The reaction mixture was aged at room temperature for 48 h, and then further aged at 100 °C for 48 h in a Teflon autoclave. The resulting products were filtered and washed with the mixture solution of distilled water and ethanol, then dried at ambient temperature.

Powder X-ray diffracion (XRD) data were obtained with a Rigaku 2400 diffractometer equipped with Cu$K\alpha$ radiation ($\lambda = 1.5418$ Å). The samples were scanned from 10° to 80° ($2\theta$). The infrared spectra in the range of 400–4000 $cm^{-1}$ were recorded by a PerkinElmer Spectra One Spectrometer with a KBr-disc technique. The surface areas were determined by BET measurements (BF, ST2000). Diffuse reflection spectra were measured by UV–vis spectrometry (PG, TU-1900) to estimate band gaps of photocatalysts. The photocatalytic reactions were carried out in a gas-closed circulation system. The photocatalyst powder (0.1 g) was dispersed in aqueous methanol solutions (volume ratio 1/20) (420 mL) by a magnetic stirrer in an inner irradiation quartz reaction cell. The light source was a 350 W high-pressure Hg lamp and 350 W high-pressure Xe lamp. The amounts of $H_2$ and $O_2$ evolved were determined by gas chromatography (Agilent, GC-6820, TCD, Ar carrier).

The electronic band-structure calculation was based on the full-potential linear-muffin-tin-orbital (FP-LMTO) method [21], which uses the generalized gradient approximation (GGA) PW91 [22], an improvement of the local spin-density approximation (LSDA) within DFT [23,24] that is known to be an efficient and accurate scheme for solving the many-electron problem of a crystal. The density of the Monkhorst–Pack $k$-point mesh are $6 \times 6 \times 6$. We construct $(2 \times 2 \times 2)$ super cells for $SrTiO_3$ and $SrTi_{1-x}Cr_xO_3$, the Cr ions are set in one of the eight $B$ sites as shown in Fig. 1. The system structures were optimized by first-principles calculations.

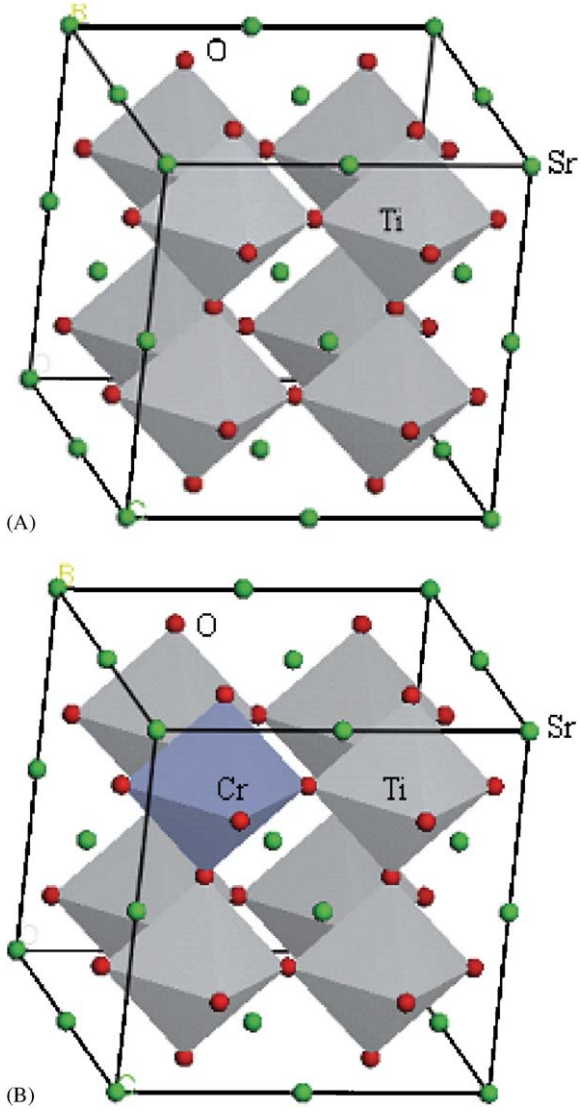


Fig. 1. Unit cells for calculations A, $SrTiO_3$; B, $SrTi_{1-x}Cr_xO_3$ ($x = 0$, 125).

## 3. Results and discussion

### 3.1. XRD and FTIR

The characterization of $SrTi_{1-x}Cr_xO_3$ crystals was carried out to clarify the factors of the increase in the photocatalytic activity by doping of chromium. The powder X-ray diffraction patterns of Fig. 2 show that the products are free of impurities. X-ray diffraction patterns of $SrTi_{1-x}Cr_xO_3$ powders are slightly shifted to higher angles with the increase in the amounts of doped chromium as shown in Fig. 3. The shift indicates that a part of chromium at least is homogeneously doped into the $SrTiO_3$ lattice. Ionic radii of six-coordinated $Cr^{3+}$ (0.62 Å) are almost the same as $Ti^{4+}$ ion (0.61 Å). In contrast, an ionic radii of $Cr^{3+}$ ion is remarkably smaller than that of 12-coordinated $Sr^{2+}$ (1.26 Å) which is at the position of A sites in perovskite structures. If $Sr^{2+}$ is replaced with $Cr^{3+}$, a large shift should be observed. Therefore, the small shifts to higher angles observed in the diffraction patterns of

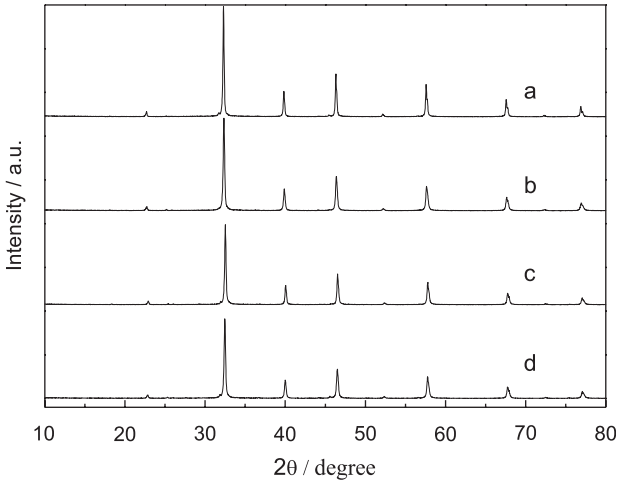


Fig. 2. X-ray diffraction patterns of (a) nondoped $SrTiO_3$ and $SrTiO_3$-doped with chromium, (b) 2%, (c) 5% and (d) 10%.

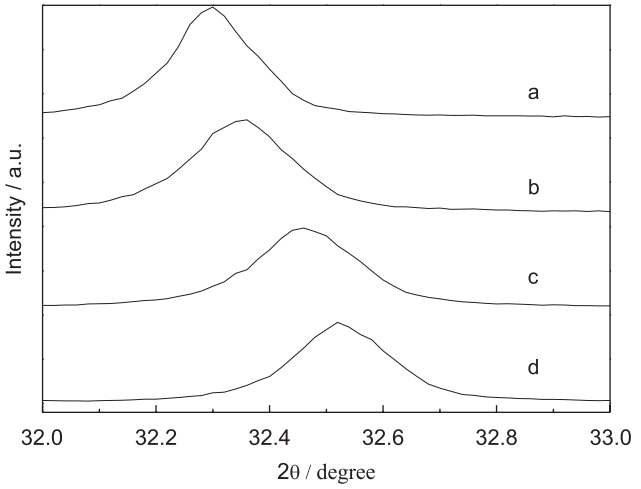


Fig. 3. X-ray diffraction peaks around 32.4° of (a) nondoped $SrTiO_3$ and $SrTiO_3$-doped with chromium, (b) 2%, (c) 5% and (d) 10%.

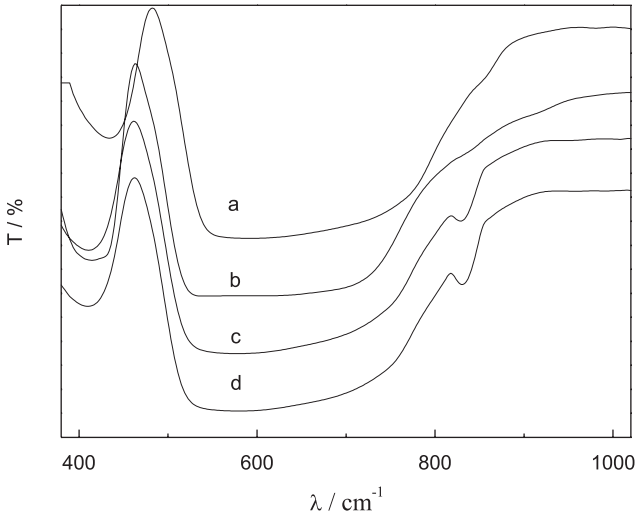


Fig. 4. IR transmission spectra of: (a) nondoped $SrTiO_3$ and $SrTiO_3$-doped with chromium, (b) 2%, (c) 5%, and (d) 10%.

$SrTi_{1-x}Cr_xO_3$ suggest the substitution of chromium ions for titanium ions in the bulk which occupy *B* sites in perovskite structures.

Fig. 4 shows IR spectra of the samples at room temperature. In the range of 400–1000 $cm^{-1}$, it is found that the IR spectra have two broad absorption bands. The two absorption bands are located at 350–450 and 500–900 $cm^{-1}$, which are attributed to $BO_6$ octahedron bending and stretching vibration, respectively [25]. The vibration frequency of $BO_6$ octahedron bending vibration absorption band decreases with the increasing of *x*. This means that the bond angle of M–O–M in $MO_6$ octahedrons increases and becomes closer to 180°. A study on luminescent properties of tantalates and niobates has shown that the closer the bond angle of M–O–M is to180°, the more the excitation energy is delocalized [26]. This indicates that the bond angle of M–O–M in $MO_6$ octahedrons is one of the important factors affecting the photocatalytic and photophysical properties of semiconductors. Cr-doped $SrTiO_3$ have the closer bond angle to 180°, which may be one of the higher activity reasons.

### 3.2. UV–vis DRS and energy structure

The onset of $SrTiO_3$ is observed in 388 nm wavelengths and the band gap is estimated to be 3.2 eV, which is a typical $E_g$ for $SrTiO_3$ [12]. The absorption patterns of $SrTi_{1-x}Cr_xO_3$ are highly dependent on the dopant concentration as shown in Fig. 5, which exhibits obvious absorption in visible light region. The charge-transfer transition between Cr ion 3*d* electrons and conduction band (CB) may explain the appearance of the red-shift. For the samples of Cr-doped $SrTiO_3$, two types of absorption are generated in the visible light region. The absorption edge of 550 nm is ascribed to the charge transfer from $Cr^{3+}$ to $Ti^{4+}$, while broad absorption ranging from 540 to 800 nm is ascribed to a *d–d* transition of $^4A_2 \rightarrow {}^4T_2$ in $Cr^{3+}$ ions in octahedral systems.

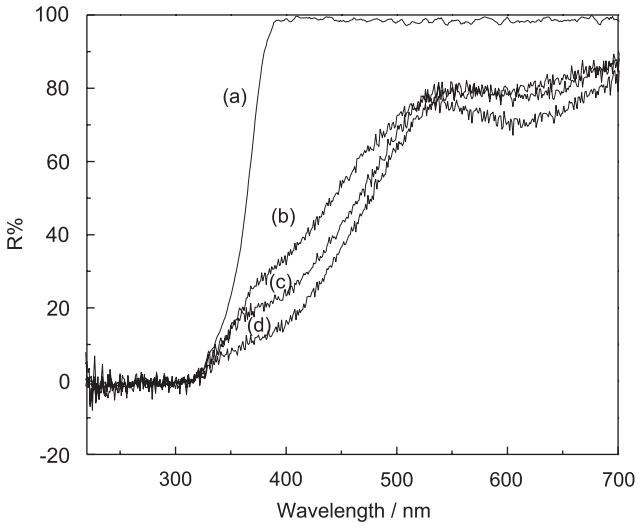


Fig. 5. UV–vis diffuse reflectance spectra of $SrTi_{1-x}Cr_xO_3$: (a) nondoped $SrTiO_3$ and $SrTiO_3$-doped with chromium, (b) 2%, (c) 5%, and (d) 10%.

### 3.3. Band structure and photoabsorption properties

The energy level and the band gap of the oxide semiconductor will play a crucial role in determining its photocatalytic activity. In the present study, the electronic structures of $SrTiO_3$ and $SrTiO_3$-doped with chromium 12.5% were investigated by DFT calculations. The total density of states (DOS) are shown in Figs. 6a and b. The bands of $SrTiO_3$ are classified into three parts. The lower-energy side in the bands for $SrTiO_3$ consisted of O 2s + Sr 5p + Ti 4p + Ti 4s hybrid orbitals. The middle part of the bands, that is, corresponding to the valence band (VB), consists of O 2*p* + Sr 5*s* + Ti 3*d* hybrid orbitals, however, O 2*p* is closer to Fermi level and contribute more electrons. The bottom of the CB is formed by the Ti 3*d* orbital. Thus, the highest occupied and the lowest unoccupied molecular orbital levels are composed of the hybrid orbitals of O

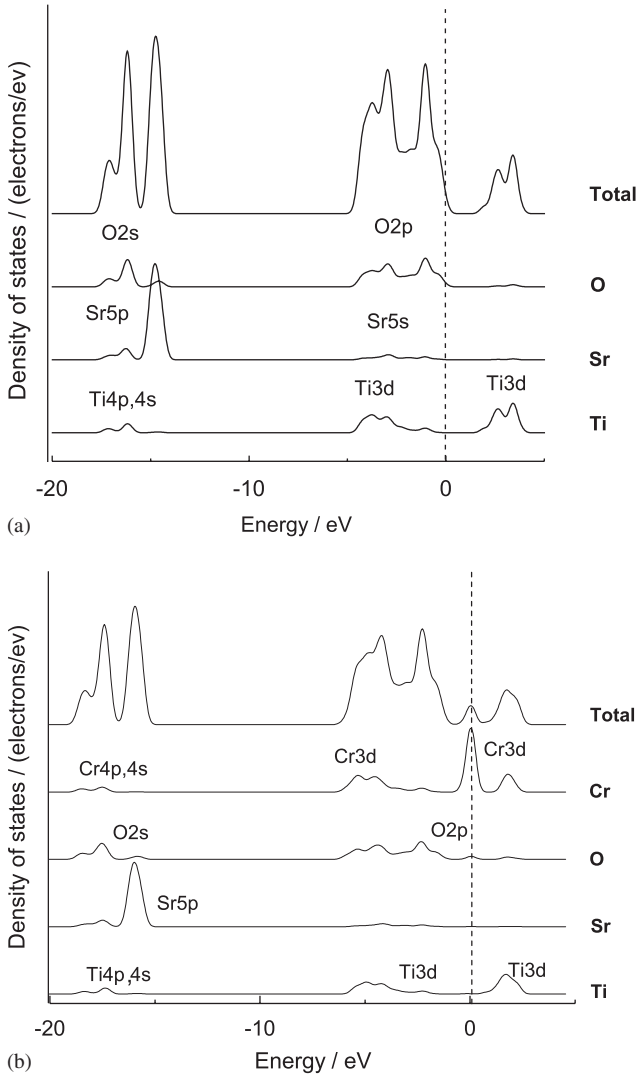


Fig. 6. The DOS of: (a) $SrTiO_3$ and (b) $SrTi_{1-x}Cr_xO_3$ ($x = 0.125$).

$2p + Sr\ 5s + Ti\ 3d$ and the Ti 3*d* orbitals, respectively. The band gap of $SrTiO_3$ is estimated to be 1.88 eV (see Fig. 7a) which is smaller than UV–vis spectra results (3.2 eV). Generally, the band gap calculated by DFT is smaller than that obtained experimentally [27,28]. This underestimation comes from some flaws in the GGA used for this calculation. As well as $SrTi_{1-x}Cr_xO_3$ ($x = 0.125$) is concerned, there are also three parts of the band. The differences are that there is an impurity state, localized Cr 3*d* band, in the middle of the $SrTi_{1-x}Cr_xO_3$ ($x = 0.125$) band gap and the CB is consists of Cr $3d + Ti\ 3d$ hybrid orbital instead. The band structure indicates that charge transfer upon photoexcitation occurs from the Cr 3*d* to the empty Cr $3d + Ti\ 3d$ hybrid orbital. This first-principles calculation result can explain the absorption peaks of UV–vis spectra. The band gap of $SrTi_{1-x}Cr_xO_3$ ($x = 0.125$) is estimated to be 0.72 eV (see Fig. 7b), which is far more narrow than that of $SrTiO_3$ (1.88 eV). This result is consistent with the large red-shift in UV–vis spectra (see Fig. 5).

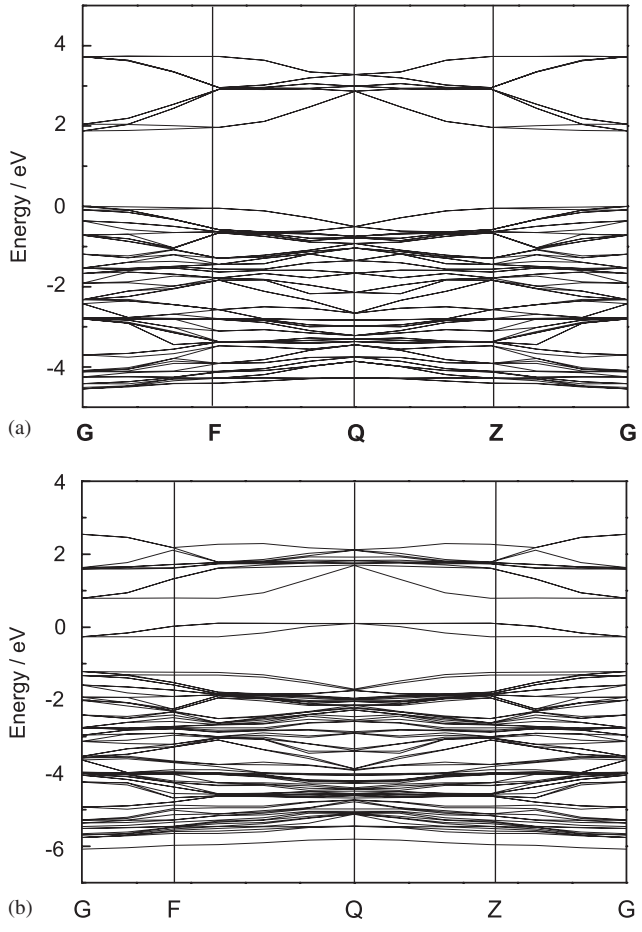


Fig. 7. The band structure of: (a) $SrTiO_3$ and (b) $SrTi_{1-x}Cr_xO_3$ ($x = 0.125$).

Table 1
Photocatalytic activities of $SrTiO_3$ doped with chromium for water splitting under UV

| Type of catalyst | Rate of gas evolution ($\mu mol\,h^{-1}\,gcat^{-1}$) | |
|---|---|---|
| | $H_2$ | $O_2$ |
| $SrTiO_3$ | 24.68 | — |
| $SrTi_{0.98}Cr_{0.02}O_3$ | 32.91 | — |
| $SrTi_{0.95}Cr_{0.05}O_3$ | 36.75 | — |
| $SrTi_{0.9}Cr_{0.1}O_3$ | 38.24 | — |

### 3.4. Photocatalytic activity for water splitting

The photocatalytic activities of chromium-doped $SrTiO_3$ both under UV and visible light are increased as shown in Tables 1 and 2. The number of photons absorbed would be increased with the increase in the amounts of chromium, resulting in the increase in the activities, which is consistent with the UV–vis spectra. The BET surface of $SrTiO_3$ ($13.62\,m^2\,g^{-1}$) and $SrTi_{1-x}Cr_xO_3$ ($12.74–13.61\,m^2\,g^{-1}$) are almost the same (see Table 3). So, the increases of photocatalytic activities for $SrTi_{1-x}Cr_xO_3$ are only caused by the chromium doping.

Table 2
Photocatalytic activities of $SrTiO_3$ doped with chromium for water splitting under visible light

| Type of catalyst | Rate of gas evolution ($\mu mol\,h^{-1}\,gcat^{-1}$) | |
|---|---|---|
| | $H_2$ | $O_2$ |
| $SrTiO_3$ | — | — |
| $SrTi_{0.98}Cr_{0.02}O_3$ | 23.03 | — |
| $SrTi_{0.95}Cr_{0.05}O_3$ | 26.46 | — |
| $SrTi_{0.9}Cr_{0.1}O_3$ | 27.92 | — |

Table 3
The BET surface of $SrTi_{1-x}\,Cr_xO_3$ ($x = 0.00, 0.02, 0.05, 0.10$)

| Type of catalyst | BET surface($m^2\,g^{-1}$) |
|---|---|
| $SrTiO_3$ | 13.62 |
| $SrTi_{0.98}Cr_{0.02}O_3$ | 12.74 |
| $SrTi_{0.95}Cr_{0.05}O_3$ | 13.61 |
| $SrTi_{0.9}Cr_{0.1}O_3$ | 13.10 |

## 4. Conclusions

The Cr-doped $SrTi_{1-x}Cr_xO_3$ powders can be synthesized at a very low temperature (100 °C) under solvothermal condition. The increase of photocatalytic activities both under UV and visible light are caused by the chromium doping. New band gap in the visible light range is obtained by chromium-doped $SrTiO_3$, which is attributed to the band transition from the Cr 3*d* to the Cr 3*d* + Ti 3*d* hybrid orbital. The absorption of visible light is of practical importance for the application of $SrTiO_3$ as photocatalyst.

## Acknowledgment

This work is supported by National Natural Science Foundation of China (Project No. 20571019): Development Program for Outstanding Young Teachers in Harbin Institute of Technology(HITQNJS.2006.028) and the Scientific Research Foundation of Harbin Institute of Technology (HIT. 2002. 54).

## References

[1] A. Kudo, Catal. Sur. Asia 7 (2003) 31–38.
[2] K.I. Shimizu, S. Itoh, T. Hatamachi, T. Kodama, M. Sato, K. Toda, Chem. Mater. 17 (2005) 5161–5166.
[3] D.W. Hwang, J.S. Lee, W. Li, S.H. Oh, J. Phys. Chem. B 107 (2003) 4963–4970.
[4] K. Sayama, K. Mukasa, R. Abe, Y. Abe, H. Arakawa, J. Photochem. Photobiol. A 148 (2002) 71–77.
[5] D. Yamasita, T. Takata, M. Hara, J.N. Kondo, K. Domen, Solid State Ionics 172 (2004) 591–595.
[6] Z.G. Zou, H. Arakaw, J. Photochem. Photobiol. A 158 (2003) 145–162.
[7] B. Sun, E.P. Reddy, P.G. Smirniotis, Appl. Catal. B 57 (2005) 139–149.
[8] D.W. Hwang, H.G. Kim, J.S. Jang, S.W. Bae, S.M. Ji, J.S. Lee, Catal. Today 93–95 (2004) 845–850.
[9] M. Kang, J. Mol. Catal. A 197 (2003) 173–183.
[10] A.D. Paola, E.G. Lopez, G. Marci, C. Martin, L. Palmisano, V. Rives, A.M. Venezia, Appl. Catal. B 48 (2004) 223–233.
[11] W.F. Yao, H. Wang, X.H. Xu, X.N. Yang, Y. Zhang, S.X. Shang, M. Wang, Appl. Catal. A 251 (2003) 235–239.
[12] K. Domen, A. Kudo, T. Onishi, J. Phys. Chem. 90 (1986) 292–295.
[13] S. Ahuja, T.R.N. Kutty, J. Photochem. Photobiol. A 97 (1996) 99–107.
[14] C. Oliva, S. Cappeli, I. Rossetti, A. Kryukov, L. Bonoldi, L. Forni, J. Mol. Catal. A 245 (2006) 55–61.
[15] S.O.Y. Matsuo, T. Omata, M. Yoshimura, J. Alloys Comps. 376 (2004) 262–267.
[16] D. Dvoranova, V. Brezova, M. Mazur, M.A. Malati, Appl. Catal. B 37 (2002) 91–105.
[17] R. Konta, T. Ishii, H. Kato, A. Kudo, J. Phys. Chem. B 108 (2004) 8992–8995.
[18] J.H. Wang, S. Yin, M. Komatsu, Q.W. Zhang, F. Saito, T. Sato, Appl. Catal. B 52 (2004) 11–21.
[19] M. Miyauchi, M. Takashio, H. Tobimatsu, Langmuir 20 (2004) 232–236.
[20] J.S. Wang, S. Yin, M. Komatsu, T. Sato, J. Europ. Ceram. Soc. 25 (2005) 3207–3212.
[21] O.K. Andersen, Phys. Rev. B 13 (1975) 3060–3083.
[22] J.P. Perdew, K. Burke, M. Ernzerhof, Phys. Rev. Lett. 77 (1996) 3865–3868.
[23] P. Hohenberg, W. Kohn, Phys. Rev. 136 (1964) B864–B871.
[24] W. Kohn, L.J. Sham, Phys. Rev. 140 (1965) A1133–A1138.
[25] S. Tan, S. Yue, Y.H. Zhang, Phys. Lett. A 319 (2003) 530–538.
[26] M. Wiegel, M.H.J. Emond, E.R. Stobbe, G. Blasse, J. Phys. Chem. Solids 55 (1994) 773–778.
[27] J. Carrasco, F. Illas, N. Lopez, E.A. Kotomin, Y.F. Zhukovskii, R.A. Evarestov, Y.A. Mastrikov, S. Piskunov, J. Maier, Phys. Rev. B 73 (2006) 064106.
[28] S. Piskunov, E. Heifets, R.I. Eglitis, G. Borstel, Comput. Mater. Sci. 29 (2004) 165–178.